

Strong suppression of star formation and spiral arm formation in disk galaxies with counter-rotating gas disks

Omima Osman ^{1*} and Kenji Bekki²

¹ *University of Khartoum - Department of Physics. Al-Gamaa Ave, Khartoum 11115, Sudan*

² *ICRAR M468 The University of Western Australia 35 Stirling Hwy, Crawley Western Australia 6009, Australia*

Accepted, Received 2005 February 20; in original form

ABSTRACT

Galaxy-wide star formation can be quenched by a number of physical processes such as environmental effects (e.g., ram pressure stripping) and supernova feedback. Using numerical simulations, we here demonstrate that star formation can be severely suppressed in disk galaxies with their gas disks counter-rotating with respect to their stellar disks. This new mechanism of star formation suppression (or quenching) does not depend so strongly on model parameters of disk galaxies, such as bulge-to-disk-ratios and gas mass fractions. Such severe suppression of star formation is due largely to the suppression of the gas density enhancing mechanism i.e spiral arm formation in disk galaxies with counter-rotating gas. Our simulations also show that molecular hydrogen and dust can be rather slowly consumed by star formation in disk galaxies with counter-rotating gas disks (i.e., long gas depletion timescale). Based on these results, we suggest that spiral and S0 galaxies with counter-rotation can have rather low star formation rate for their gas densities. Also we suggest that a minor fraction of S0 galaxies have no prominent spiral arms, because they have a higher fraction of counter-rotating gas. We predict that poststarburst ‘E+A’ disk galaxies with cold gas could have counter-rotating gas.

Key words: galaxies: evolution– galaxies: star formation– galaxies: ISM

1 INTRODUCTION

Since disk galaxies with counter-rotating components were first discovered in 1987 by Galletta, the origin of them has been discussed extensively by observational and theoretical studies¹. Despite the fact that counter-rotation has been observed across the whole Hubble sequence, counter-rotation is more frequent in early-type disk galaxies. A statistical study by Bureau & Chung (2006) found that (i) 60 galaxies classified as S0 have a significant amount of ionized gas and (ii) 14 of the S0s with ionized gas have counter-rotating ionized gas, representing $(23\pm 5)\%$. This result was obtained by merging samples of Bertola et al. 1992, Kuijken et al. 1996, Kannappan & Fabricant 2001, Pizzella et al. 2004 and Bureau & Chung 2006. More recent study by Davis et al. (2011) have provided strong evidence on favor of the external origin of the counter-rotating gas in early-type galaxies. While Sarzi et al. 2006 did not rule out the internal ori-

gin of the misaligned gas. Jin et al. 2016 found that about 85% of their sample of galaxies with misaligned gas lay in the green valley and red sequence. Kannappan & Fabricant (2001) and Pizzella et al. (2004) have addressed the counter-rotation frequency in spiral galaxies with samples of 38 S0/a-Scd and 50 S0/a-Scd galaxies, respectively. Kannappan & Fabricant set an upper limit of 8% on the fraction of spirals that host counter-rotating gas, whereas Pizzella et al. (2004) found less than 12% of their galaxies sample hosting counter-rotating gas.

Theoretical studies showed that secondary slow episodic and continuous infall of non-clumpy gas is the most viable mechanism to form massive counter-rotating disk in spiral galaxies according to the numerical simulation results of Thakar & Ryden (1996). Major mergers between spirals of similar masses are unlikely to form disk galaxies with counter-rotation, because they can completely destroy the original disks (Thakar & Ryden 1996; Mapelli et al. 2015; Bassett et al. 2017). Internal processes that may lead to counter-rotation were also discussed by a number of authors (e.g., Evans & Collett 1994, Wozniak & Pfenniger 1997). Other interesting theoretical studies found that counter-

* E-mail: omima.osman@uwa.edu.au

¹ For a list of counter-rotating galaxies refer to Corsini & Bertola 1998 and to Corsini 2014 for a review

Table 1. The basic model parameters for disk galaxies.

Model ID ^a	M_s ^b	M_g ^c	f_g ^d	f_b ^e	V_c ^f	ρ_{th} ^g
M1	6.0	0.6	0.1	0.17	S	100
M2	6.0	0.6	0.1	0.17	C	100
M3	0.6	3.0	5.0	0	S	100
M4	0.6	3.0	5.0	0	C	100
M5	1.8	1.8	1.0	0	S	100
M6	1.8	1.8	1.0	0	C	100
M7	6.0	0.6	0.1	0	S	100
M8	6.0	0.6	0.1	0	C	100
M9	4.8	1.8	0.37	0.17	S	100
M10	4.8	1.8	0.37	0.17	C	100
M11	3.0	0.6	0.2	1.0	S	100
M12	3.0	0.6	0.2	1.0	C	100
M13	4.8	1.8	0.37	0	S	100
M14	4.8	1.8	0.37	0	C	100
M15	6.0	0.3	0.05	0.17	S	100
M16	6.0	0.3	0.05	0.17	C	100
M17	6.0	0.3	0.05	0.17	S	10
M18	6.0	0.3	0.05	0.17	C	10
M19	6.0	0.6	0.1	0.17	S	10
M20	6.0	0.6	0.1	0.17	C	10
M21	6.0	0.6	0.1	0.17	S	30
M22	6.0	0.6	0.1	0.17	C	30
M23	6.0	0.6	0.1	0.17	S	100
M24	6.0	0.6	0.1	0.17	C	100

^a The model M23 and 24 are the same as M1 and M2, respectively, but star formation rate is assumed to depend on total gas density.

^b The initial total mass of a stellar disk in units of $10^{10} M_\odot$.

^c The initial total mass of a gas disk in units of $10^{10} M_\odot$.

^d Gas fraction, measured as the initial mass ratio of gas to stars in a disk galaxy.

^e The bulge-to-disk mass-ratio in a disk galaxy.

^f ‘S’ and ‘C’ represents the standard rotation (i.e., co-rotation) and counter-rotation, respectively.

^g The threshold gas density for star formation in units of cm^{-3} .

rotating stellar disks develop one-armed spiral waves due to two-stream instability, (e.g., Lovelace et al. 1997, Comins et al. 1997). Furthermore, Lovelace et al. (1997) found that, for co-rotating stellar disk with less than 50% mass fraction in counter-rotating stars/gas, the strongest amplification occurs for the first mode ($m = 1$), which corresponds to one-armed leading waves. Smaller amplification can be seen for the second mode ($m = 2$), i.e., two-armed trailing waves.

The dynamics of gas and stars in galaxies is a very important driver of galaxy formation and evolution. Accordingly, we expect that counter-rotating components, in particular, gaseous counter-rotation can have significant influence on galactic stellar and gas dynamics, which can, in turn, influence star formation and H_2 formation. However, the above-mentioned previous studies did not investigate this issue. H_2 gas, which is the building block of molecular clouds where star formation is ongoing, can be formed on the surfaces of dust grains from neutral hydrogen. Star formation and its feedback effects (e.g., supernova explosions) can destroy the interstellar dust grains and therefore influence H_2 formation processes. Thus, both the formation and evolution of dust and that of molecular gas needs to be investigated self-consistently so that the influence of counter-rotating gas on galaxy-wide star formation can be adequately addressed.

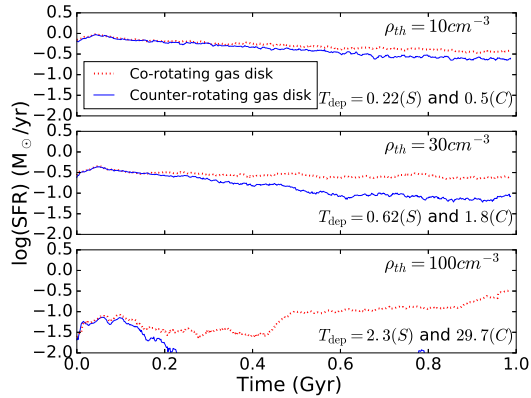


Figure 1. Time evolution of SFRs in co-rotating (‘S’) models (from the top) M19, M21 and M1 (red dotted) and counter-rotating (‘C’) models M20, M22 and M2 (blue solid) for $\rho = 10$ (top) 30 (middle), 100 cm^{-3} (bottom). Gas depletion times (T_{dep} ($\times 10^{10} \text{ yr}$) at the initial time for co-rotating models and the final time for the counter-rotating models) are also indicated for each model.

Thus the purpose of this paper is to investigate whether star formation rates (SFRs) can be severely suppressed in disk galaxies, if the gaseous components are counter-rotating with respect to their stellar disks. We also discuss how the formation of molecular hydrogen (H_2) on dust grains can be influenced by counter-rotating kinematics of gas in detail. The physical properties of H_2 formation and star formation in counter-rotating gas disks were addressed observationally by Betttoni et al. (2001). However, we present the first theoretical study on this issue in the present study.

2 THE MODEL

In order to derive star formation rates (SFRs) of disk galaxies with co-rotating or counter-rotating gas disks, we adopt our original simulation code that has been recently developed to analyze the evolution of dust, metal, molecular hydrogen in galaxies (Bekki 2013, 2015, hereafter B13, B15). We here describe them briefly, because the details of the code are already given in Bekki (B13, B15). The code is based on the smoothed-particle hydrodynamics (SPH) method, and it includes various physical processes of interstellar medium and stellar evolution so that we can investigate various processes.

A disk galaxy is assumed to consist of dark matter halo, stellar disk, gas disk and stellar bulge with the total masses being denoted as M_h , M_s , M_g , and M_b , respectively. The mass-ratio of gas disk to stellar disk is denoted as f_g and considered to be a key parameter for the time evolution of SFRs and molecular gas fraction. The initial density profile of dark matter halo in a disk galaxy is modeled using the density distribution of the NFW halo (Navarro et al. 1996) suggested from CDM simulations. The c -parameter ($c = r_{vir}/r_s$, where r_{vir} and r_s are the virial radius of a dark matter halo and the scale length, respectively) and r_{vir} are chosen appropriately by using recent predictions from cosmological simulations (Neto et al. 2007).

We adopt the Hernquist density profile for the bulge of a disk galaxy and the bulge mass fraction (M_b/M_s) is a free parameter ranging from 0 to 1. The size (R_b) and

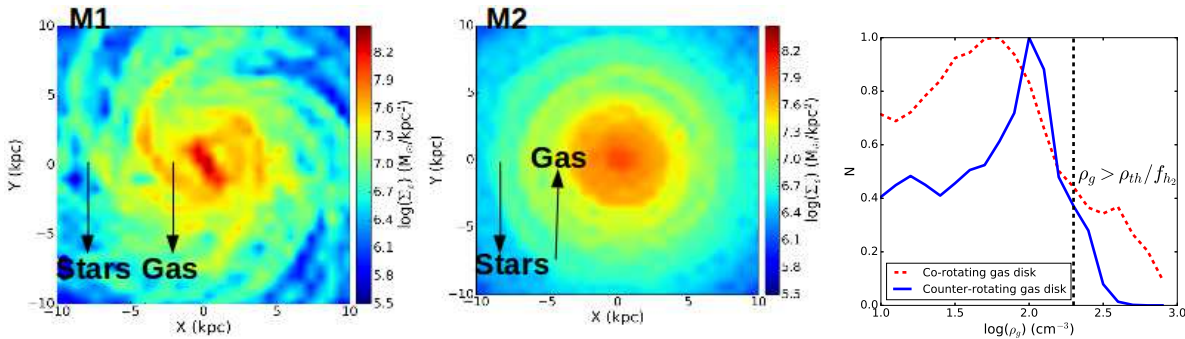


Figure 2. The surface mass density of the gas disk (Σ_g , at $T = 0.98$ Gyr) in logarithmic scale projected onto xy plane for the co-rotating model M1 (left) and the counter-rotating model M2 (middle). The black arrows show the rotation direction for stars and gas. The number of particles as a function of the logarithm of the volume density (right). Red dashed and blue solid lines represent M1 and M2, respectively, and the black dashed vertical line indicates the threshold H_2 gas density for star formation, in the right panel. This can be compared with the results in Fig. 4 of Martig et al. (2013).

the mass of the bulge has the following scaling relation that can reproduce the properties of the Galactic bulge: $R_b = 2 \left(\frac{M_b}{10^{10} M_\odot} \right)^{0.5} \text{kpc}$. The radial (R) and vertical (Z) density profiles of the stellar disk are assumed to be proportional to $\exp(-R/R_0)$ with scale length $R_0 = 0.2R_s$ and to $\text{sech}^2(Z/Z_0)$ with scale length $Z_0 = 0.04R_s$, respectively. The gas disk with a size of R_g has the radial and vertical scale lengths of $0.2R_g$ and $0.02R_g$, respectively. Since we investigate disk models with M_h similar to that of the Galaxy (i.e., $M_h = 10^{12} M_\odot$), the exponential disk has $R_s = 17.5$ kpc for all models in the present model. The initial Toomre’s parameter Q is set to be 1.5 for gas and stars and the vertical velocity dispersion at a given radius is set to be 0.5 times as large as the radial velocity dispersion at that point so that the dynamical equilibrium in the vertical direction can be achieved.

A gas particle is assumed to be converted into a new star, if the local H_2 density ($f_{H_2} \rho_g$ where f_{H_2} and ρ_g are the H_2 mass fraction and gas density, respectively) exceeds a threshold density (ρ_{th}) and we investigate the models with $\rho_{th} = 10, 30$ and 100 cm^{-3} . These are H_2 -dependent SF model, and we also investigate H-dependent one in which ρ_g should be higher than ρ_{th} . We adopt these values, because our previous numerical simulations of galaxy evolution with dust demonstrated that the models with the above values can explain the observed SFR- Σ_g relation (See Fig. 3 in Yozin & Bekki 2014 for the case of the Magellanic Clouds). We assume that $\text{SFR} \propto \rho_g^{\alpha_{sf}}$ ($\alpha_{sf} = 1.5$) in the present study. Chemical enrichment processes, dust formation and evolution in ISM and SN feedback effects are included in the same way as B13 and 15.

We investigate disk models with co-rotating (referred to as ‘standard’ rotation and labelled as ‘S’ for convenience) and counter-rotating (‘C’) gas disks for a given set of disk parameters. By comparing between the two models, we try to understand how counter-rotating gas can influence dynamics and star formation histories of disk galaxies. We show the results for only 24 models in the present study and Table 1 describes the model parameters for each of the ‘S’-‘C’ pairs. The total number of particles used for a simulation is 1033400 for a fiducial model (M1 and M2) and different initial gravitational softening lengths (ϵ) are allocated for

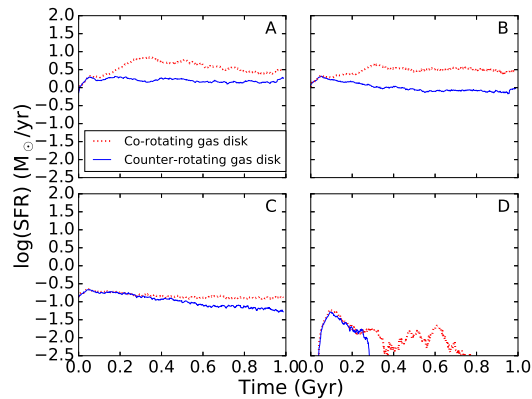


Figure 3. The time evolution of SFRs in models; (A) M5 and M6, (B) M9 and M10, (C) M17 and M18, (D) M11 and M12. Red dotted lines and blue solid lines represent co-rotating and counter-rotating models, respectively.

different four components: $\epsilon = 2.1 \text{ kpc}$ and 0.26 kpc for dark matter and baryonic components.

3 RESULTS

Fig. 1 shows the time evolution of the SFRs in the co-rotating models M1, M19 and M21 and counter-rotating models M2, M20 and M22. All the co-rotating and counter-rotating models have the same parameters except for the SF density threshold, $\rho_{th} = 10, 30, 100 \text{ cm}^{-3}$ (top to bottom). The SFR in all models with counter-rotating gas disk is suppressed in comparison with co-rotating gas disk models. Changing the SF density threshold only changes the magnitude of suppression: As we go to higher ρ_{th} , SF suppression becomes stronger. This result can also be seen in models M23 and M24. Gas depletion times (T_{dep}) are also indicated for the different models (see e.g. Martig et al 2013, Davis et al. 2013, Davis & Bureau 2016, for the T_{dep} calculation). To understand the reason behind this suppression we studied the time evolution of the gas surface density distribution (Σ_g) at $T = 0.49$ Gyr and $T = 0.98$ Gyr. The 2D distribution of the gas disks in models M1 with co-rotation gas (left), M2 with counter-rotation gas (middle) and the number of particles as a function of the logarithm of the

volume density of the two models (right) at time $T = 0.98$ Gyr are shown in Fig. 2. The surface mass density of the gas (Σ_g) in logarithmic scale is plotted for the two models. Clearly, the 2D distribution shows the formation of gas concentrations around the spiral arms and within the stellar bar for the co-rotating gas disk, whereas the spiral arms and bar completely fail to form in this case of counter-rotating disk. Since high fraction of star formation takes place around spiral arms, due to the enhanced gas density by the arms, the lack of those arms leads to suppression in the SFRs. The stellar bar, which was formed as the result of the dynamical evolution of the system, can drive rapid inward transfer to the inner region of the stellar disk so that star formation can become active there. The volume density as well shows the domination of the co-rotating model in two density regimes, below $10^{1.8}$ and above $10^{2.4}$ cm^{-3} , however, the second regime is the one relevant for star formation. The regime over which counter-rotating model is dominant, most probably, is the one in which H_2 is forming (see fig. 4).

Fig. 3 shows the time evolution of SFRs for co-rotating and counter-rotating gas disks in models with different model parameters. The SFR suppression for the counter-rotating gas disks is evident in all models even in the cases in which models with counter-rotating gas disks show spiral structure. In 60% of the counter-rotating models in this paper, no spiral arms or bars were formed. The rest of the models (40%) show weak spiral structures that are regarded as ‘leading’ arms rather than ‘trailing’ ones (with respect to stellar rotation). Models in (A) exhibit a kind of clumpy structure in the co-rotating case (M5) and smoother structure with spirals in the counter-rotating case (M6). For both cases of co-rotation M9 and counter-rotation M10 in (B), spiral arms can be formed, however, with smoother structure in the case of M10. Models M17 and M18 in (C) and models M11 and M12 in (D) show spiral structure for the co-rotating gas disk, while the spiral structure completely fails to form in counter-rotation case. Star formation proceeded with significantly lower rates in the model M11 with big bulge, while star formation is truncated within ~ 0.3 Gyr for the model M12 with counter-rotating gas.

Previous observations revealed physical correlations between H_2 properties (e.g., mass and H_2/HI ratio) and galactic basic physical properties (mass, size, morphological types in disk galaxies with co-rotating and counter-rotating disks (e.g., Casoli et al. 1998). Fig. 4 shows the time evolution of H_2/HI ratio and the time evolution of the total gas in models M1 and M2. The gas consumption is slower in the counter-rotation case due to the lower star formation rate (due to the lack of the mechanism that enhances gas density, i.e., the spiral arms). Owing to the slow gas consumption in M2, H_2 formation on dust grains can continue and consequently the H_2 -to- HI -ratio becomes higher in M2 ($M_{\text{H}_2} = 3.07 \times 10^9, 3.46 \times 10^9 M_\odot$ at $T = 0.98$ Gyr for models M1 and M2 respectively). Although possible enhancement of the HI to H_2 conversion efficiency in disk galaxies with counter-rotation gas was already speculated by Bettoni et al. (2001), the present study first demonstrates higher H_2 -to- HI -ratios in simulated disks with counter-rotation. Since H_2 forms exclusively on the surface of dust grains in the present model, its higher abundance in counter-rotating gas disks indicates quieter and milder environment with less dust destruction

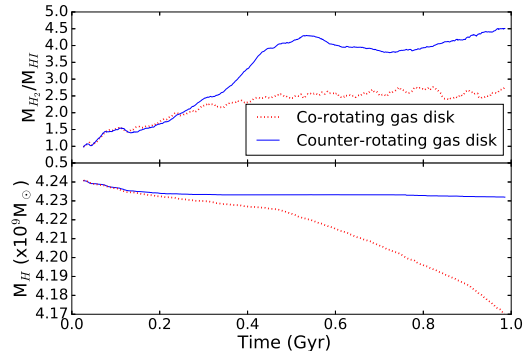


Figure 4. The time evolution of the ratio of molecular hydrogen to atomic hydrogen, upper panel, and that of the total gas, lower panel. Red dotted lines and blue solid lines represent M1 and M2, respectively.

processes. Indeed, the final dust masses in M1 and M2 are 7.87×10^7 and $9.45 \times 10^7 M_\odot$, respectively.

Fig. 5 shows the mean SFR in disks with counter-rotating gas disks as a function of that in disks with co-rotating gas disks. Notably, all the points lie below the line at which the SFR mean for the co-rotating disks is equal to that for counter-rotating disks. We have also found that these results can be seen in the models with big bulges ($f_b = 1$ and small gas fractions $f_g = 0.05$). These therefore confirm that galaxy-wide star formation can be strongly suppressed in disks with counter-rotating gas for different galaxy-types. The higher dust amount in counter-rotating gas disks, owing to the inefficient dust destruction mechanisms, allow higher amounts of HI gas to combine into H_2 gas. Despite this fact, the SFR is lower in all the different cases. This is mainly because spiral-arm formation, which can induce the formation of local high-density regions, is severely suppressed in the models with counter-rotating gas. Fig. 5 also shows that the depletion time scale, which is defined as $M_{\text{H}_2}/\text{SFR}$, is longer in our counter-rotating models in comparison with the recent observational results by Martig et al. (2013).

4 DISCUSSION AND CONCLUSIONS

There are many different mechanisms that lead to star formation quenching in galaxies, such as environmental effects (e.g., ram pressure stripping), supernovae feedback and AGN feedback. Here we have shown a new mechanism for severe suppression of star formation in disk galaxies with counter-rotating gas disks. To address the validity and efficiency of this mechanism, we have investigated 24 models with different model parameters for disk galaxies. We have found that suppression of star formation can be seen in almost all models with different bulge-to-disk-ratios, gas mass fractions and threshold gas densities for star formation. The derived rather low SFRs in disk galaxies with counter-rotating gas is due to the lack of gas density enhancing mechanism, i.e., spiral arms, which can trigger the formation of massive stars in disk galaxies. Owing to the lack of spiral arms, gas densities can not be locally so high in counter-rotating gas. In most of the present counter-rotating models ($\sim 60\%$), both spiral arms and bars fail to form within a time scale of 1 Gyr: these models show either very smooth density distributions or weak ring-like structures. It is surprising that spiral arm formation is completely suppressed in

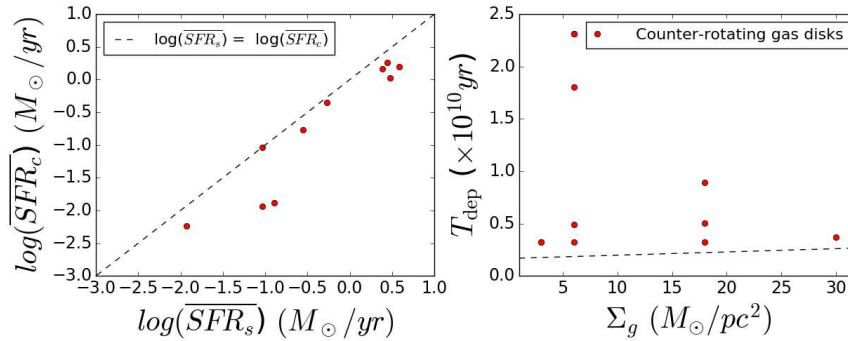


Figure 5. The mean SFR (\overline{SFR}) for counter-rotating ('c') gas disk as a function of \overline{SFR} of disk galaxies with co-rotating ('s') disk (left) and the gas depletion time scale (T_{dep}) as a function of Σ_g (right). The dashed line is $T_{\text{dep}} = 0.17 \times \Sigma_g^{0.13}$, from Martig et al. 2013.

gas-poor disk galaxy models in the present study. Probably, a physical mechanism of spiral arm formation (e.g., swing amplification mechanism) does not operate efficiently, if the counter-rotating gas has small fraction (f_g). These results strongly suggest that counter-rotation is a viable explanation for the lack of spiral arms in a fraction of the gas bearing S0 galaxies. Recent numerical simulations of S0 formation with counter-rotation have discussed the origin of counter-rotating gas (e.g., Mapelli et al. 2015; Bassett et al. 2017), they did not discuss why spiral arms can not be generated in S0s. The present study, for the first time, provides a physical explanation for the lack of spiral arms in S0s with counter-rotating gas.

'E+A' galaxies are galaxies that have spectra with strong optical absorption lines but no or little optical emission lines, which indicates that these E+A galaxies have a significant fraction of young A-type stellar population yet low star formation rate. The importance of those systems comes from their suggestive transition state between disk dominated, star forming galaxies and quiescent, passive spheroids (e.g., Zabludoff et al. 1996). Zwaan et al. 2013 and French et al. 2015 looked at the gas content (HI and H₂, respectively) of the E+A disk galaxies. Zwaan et al. found that the gas fraction ranging from 0.01 to 0.1 whereas French et al. (2015) suggested that the low SFRs in E+As with significant fractions of H₂ can not be due to lack of gas. There has been some proposals to explain the presence of HI gas with the lack of star formation (Buyle et al. 2006, Pracy et al. 2014). In this study we have found that despite the existence of gas, star formation is suppressed severely. Accordingly we suggest that some E+As with cold gas could potentially have counter-rotating gas disks.

5 ACKNOWLEDGMENT

We are grateful to the referee for constructive and useful comments that improved this paper.

REFERENCES

Bassett R., Bekki K., Cortese L., Couch W. J., 2017, arXiv, arXiv:1704.08434

- Bekki K., 2013, MNRAS, 432, 2298
 Bekki K., 2015, MNRAS, 449, 1625
 Bertola F., Buson L. M., & Zeilinger W. W., 1992, ApJ, 401, L79
 Bettoni D., Galletta G., Garcia-Burillo S., & Rodriguez-Franco A., 2001, A&A, 374, 421
 Bureau M., & Chung A., 2006, MNRAS, 366, 182
 Buyle P., Michielsen D., De Rijcke S., et al., 2006, ApJ, 649, 163
 Casoli F., Sauty S., Gerin M., et al., 1998, A&A, 331, 451
 Comins N. F., Lovelace R. V. E., Zeltwanger T., Shorey P. A., 1997, ApJ, 484, L33
 Corsini E. M., 2014, ASP Conference Series Vol. 486, 51
 Corsini E. M., & Bertola F., 1998, J. Korean Phys. Soc., 33, 574
 Davis T. A., Alatalo K., Sarzi M., et al., 2011, MNRAS, 417, 882
 Davis T. A., Young L. M., Crocker A. F., et al., 2013, MNRAS, 429, 534
 Davis T. A., & Bureau M., 2016, MNRAS, 457, 272
 Evans N. W., & Collett J. L., 1994, ApJ, 420, L67
 French K. D., Yang Y., Zabludoff A., et al., 2015, ApJ, 801, 1
 Galletta, G., 1987, ApJ, 318, 531
 Jin Y., Chen Y., Shi Y., 2016, MNRAS, 463, 913
 Kannappan S. J., & Fabricant D. G., 2001, AJ, 121, 140
 Kennicutt, R. C. Jr., 1998, ApJ, 498, 541
 Kuijken K., Fisher D., & Merrifield M.R., 1996, MNRAS, 283, 543
 Lovelace R. V. E., Jore K. P., Haynes M. P., 1997, ApJ, 475, 83L
 Mapelli M, Rampazzo R., Marino A., 2015, arXiv, arXiv:1501.00016
 Martig M., Crocker A. F., Bournaud F., et al., 2013, MNRAS, 432, 1914
 Navarro J. F., Frenk C. S., White S. D. M., 1996, ApJ, 462, 563
 Neto A. F., Gao L., Bett P., 2007, 381, 145
 Pizzella A., Corsini E. M., Vega Beltran J. C., & Bertola

- F., 2004, *A&A*, 424, 447
Pracy M. B., Owers M. S., Zwaan M., et al., 2014, *MNRAS*, 443, 388
Sarzi M., Falcon-Barroso J., Davies R. L., et al., 2006, *MNRAS*, 366, 1151
Thakar A., & Ryden B., 1996, *ApJ*, 461, 55
Wozniak H., & Pfenniger D., 1997, *A&A*, 317, 14
Yozin C. & Bekki K., 2014, *MNRAS*, 443, 522
Zabludoff A. I., Zaritsky D., Lin H., et al., 1996, *ApJ*, 466, 104
Zwaan M. A., Kuntschner H., Pracy M. B., Couch W. J., 2013, *MNRAS*, 432, 492